Lawrence Berkeley National Laboratory
LBL Publications

Title
BilboMD: a web-accessible SAXS and AlphaFold-guided modeling pipeline

Permalink
https://escholarship.org/uc/item/41k4q9rc

Journal
Nucleic Acids Research, 54(W1)

ISSN
0305-1048

Authors
Classen, S
Del Mundo, J
Kulkarni, D
et al.

Publication Date
2026-07-07

DOI
10.1093/nar/gkag377

Copyright Information
This work is made available under the terms of a Creative Commons Attribution License, available at https://creativecommons.org/licenses/by/4.0/

Peer reviewed

eScholarship.org Powered by the California Digital Library
University of California

Nucleic Acids Research, 2026, **54**, W216–W225
https://doi.org/10.1093/nar/gkag377
Advance access publication date: 27 April 2026
Web Server issue

BilboMD: a web-accessible SAXS and AlphaFold-guided modeling pipeline

Scott Classen [1,*], Joshua Del Mundo [1], Dhruva Kulkarni [2], Shreyas Prabhakar [2], Alan Hicks [3], Michal Hammel [1,*]

[1]Molecular Biophysics and Integrated Bioimaging, Lawrence Berkeley National Laboratory, Berkeley, CA, 94720, United States
[2]NERSC, Lawrence Berkeley National Laboratory, Berkeley, CA, 94720, United States
[3]Neutron Scattering Division, Oak Ridge National Laboratory, Oak Ridge, TN, 37830, United States

*To whom correspondence should be addressed. Email: sclassen@lbl.gov
Correspondence may also be addressed to Michal Hammel. Email: mhammel@lbl.gov

Abstract

BilboMD is a web-accessible platform that facilitates integrative modeling of flexible macromolecules using experimental small-angle X-ray and neutron scattering data. BilboMD combines a browser-based interface with high-performance back-end services hosted locally at the SIBYLS beamline and at the National Energy Research Scientific Computing Center (NERSC). BilboMD guides users through a workflow that includes preparing compatible input files, conformational sampling through molecular dynamics (MD) simulations, small-angle X-ray scattering (SAXS) fitting with FoXS, and establishing multi-state models with MultiFoXS. Input assistants (Inp Jiffy and PAE Jiffy) streamline the process of defining rigid and flexible regions for conformational sampling, including automatic inference from AlphaFold PAE matrices. All analyses are containerized to ensure reproducibility, with job metadata and provenance stored in a central database. By leveraging GPU-enabled MD engines, such as OpenMM (on NERSC resources), BilboMD significantly accelerates conformational sampling and expands the set of models used for SAXS fitting. The platform reduces technical barriers for non-specialists while providing API access for advanced users to automate and integrate with custom workflows. Thus, BilboMD democratizes ensemble-based SAXS modeling, accelerates high-throughput SAXS/small-angle neutron scattering analysis, and lays the groundwork for future integration of AI-driven structure prediction with experimental scattering data. It is freely available without a login requirement at https://bilbomd.bl1231.als.lbl.gov.

Graphical abstract

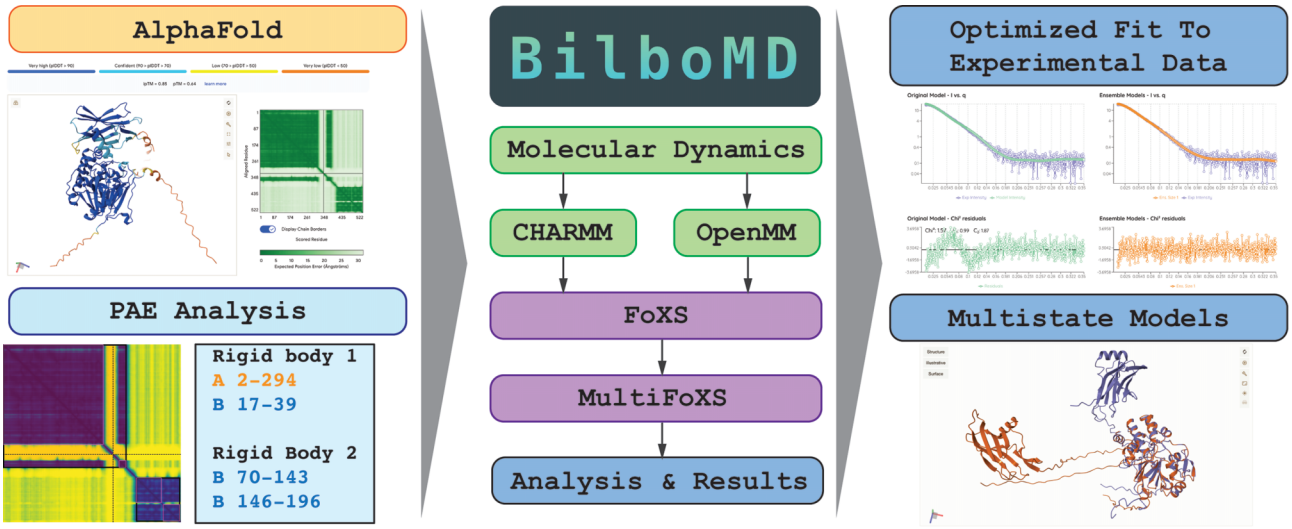

Introduction

Small-angle X-ray scattering (SAXS) has become an indispensable tool for studying biological macromolecules in solution. Unlike macromolecular X-ray crystallography (MX) or cryogenic electron microscopy (cryo-EM), which provide high-resolution static structures, SAXS, in combination with

Received: February 5, 2026. **Revised:** March 26, 2026. **Accepted:** April 12, 2026
© The Author(s) 2026. Published by Oxford University Press.
This is an Open Access article distributed under the terms of the Creative Commons Attribution-NonCommercial License (https://creativecommons.org/licenses/by-nc/4.0/), which permits non-commercial re-use, distribution, and reproduction in any medium, provided the original work is properly cited. For commercial re-use, please contact reprints@oup.com for reprints and translation rights for reprints. All other permissions can be obtained through our RightsLink service via the Permissions link on the article page on our site—for further information please contact journals.permissions@oup.com.

Downloaded from academic.oup.com/nar/article/54/W1/W216/8662889 by guest on 17 November 2026

atomistic modeling, enables the determination of ensemble structures under near-physiological conditions. Biological SAXS can elucidate the overall size, shape, and conformational variability of proteins, nucleic acids, and their complexes, making it particularly valuable for characterizing flexible macromolecules in solution that are difficult to study by traditional static high-resolution techniques [1]. SAXS parameters such as the radius of gyration (R_g), volume of correlation (V_c) [2], maximum dimension (D_{max}) from the pair-distance distribution function $P(r)$ [3] can be derived directly from SAXS profiles, providing important constraints for modeling macromolecular conformations.

The wide applicability of SAXS has been expanded by advances in synchrotron instrumentation, detector technology, and automated data reduction pipelines [4–6]. These progressions have enabled the high-throughput collection of scattering profiles [7, 8]. However, interpreting SAXS data remains challenging due to an inherently low information content. To gain more detailed structural insights, experimental SAXS data should be compared with theoretical profiles calculated from atomistic models [9, 10].

SAXS calculators like FoXS [9, 11] or CRYSOL [10] can be combined with conformational sampling that generates and assesses models, ranging from rigid-body fitting of atomic coordinates to molecular dynamics (MD)-based refinement [12, 13]. This integration is particularly important for flexible/dynamic macromolecules, in which multiple conformational states coexist in solution and influence the experimental SAXS profile. SAXS has become a powerful complement to high-resolution structural techniques such as MX or cryo-EM, providing ensemble-level information that better captures the allostery and dynamics of biological molecules [14–19]. The growing use of SAXS in integrative structural biology has spurred the development of software pipelines [15, 20] that simplify SAXS data analysis and make advanced modeling tools available to a broader community of researchers.

Despite the widespread availability of SAXS data analysis packages [21, 22], most SAXS-based atomistic modeling remains a major barrier to broader adoption. Many require local installation of complex software with numerous dependencies, which can be difficult for non-expert users to set up and maintain. The learning curve for using these tools effectively is steep, as they demand knowledge of command-line interfaces, scripting, and various file formats. Additionally, reproducibility is hindered by differences across computing environments: analyses performed on personal workstations are hard to replicate elsewhere, and software versions or parameter choices are often not systematically recorded. As a result, SAXS modeling workflows tend to be fragmented, inaccessible to non-specialists, and challenging to reproduce across different research groups.

To address these challenges, we developed BilboMD, a web-accessible pipeline that enhances SAXS-guided atomistic modeling by making it more accessible, reproducible, and scalable. By deploying BilboMD at the National Energy Research Scientific Computing Center (NERSC), BilboMD combines the benefits of high-performance GPU computing with an easy-to-use browser interface. This deployment maintains consistent software environments through containerization and grants access to powerful GPU-enabled resources. These features enable direct integration of AlphaFold (AF) [23, 24] predictions into SAXS modeling workflows and facilitate the use of modern, GPU-accelerated MD engines, such as OpenMM

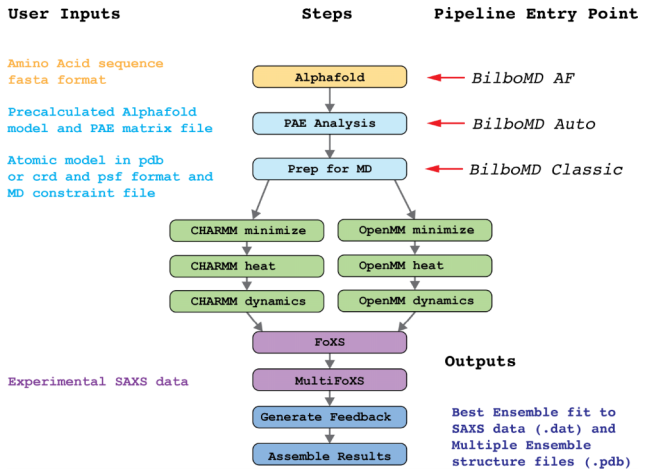

Figure 1. Schematic of BilboMD pipelines. User-provided inputs are summarized on the left side, and entry points for BilboMD AF, BilboMD Auto, and BilboMD Classic are indicated on the right. Individual steps of the modeling pipeline are shown in the middle with a user-selectable MD engine (CHARMM or OpenMM) indicated by the parallel green MD steps. Outputs are indicated at the bottom right.

Pipeline/Jiffy	SAXS/SANS data	Initial model	AlphaFold PAE	MD Constraints	Sequence	Outputs
file format	.dat	.pdb,.crd,.psf	.json	CHARMM .inp	fasta	
BilboMD Classic	✓	✓*		✓		Best model fit (.dat) and ensemble structure (.pdb) files
BilboMD Auto	✓	✓	✓			
BilboMD AF	✓				✓	
BilboMD SANS	✓	✓				
Inp Jiffy		✓				Molecular Dynamics Constraints (.inp)
PAE Jiffy		✓	✓			

Figure 2. Summary of inputs and outputs of each of the pipelines and the two Jiffys available on the BilboMD web app. *can alternatively use `*.crd` and `*.psf` files obtained from CHARMM-GUI.

[25], thereby significantly reducing conformational sampling time. Overall, BilboMD lowers technical barriers for end-users while expanding SAXS analysis capabilities to include atomistic modeling that would otherwise be difficult on standard desktop systems.

Materials and methods

Pipeline structure

BilboMD offers several pipelines (Fig. 1). Pipeline selection depends on the available inputs and desired modeling modality. Some pipelines require specific computing hardware; for example, the BilboMD AF pipeline, which uses AlphaFold, requires GPU resources and is currently only accessible on the NERSC-deployed instance.

The primary required inputs are experimental SAXS/small-angle neutron scattering (SANS) data and an atomistic model of the protein/DNA/RNA or its complex (Fig. 2). The initial atomistic model can be provided as a PDB coordinate file or as a CRD file generated by CHARMM-GUI [26]. The initial structure can be experimental or from a structure prediction such as an AlphaFold model. For BilboMD AF, the user should provide the protein sequence of each component as a FASTA-like single amino acid string. BilboMD AF is capable of processing monomers and both homo- and hetero-multimers but is currently limited to proteins since the underlying predictions are using AlphaFold2. The BilboMD AF pipeline performs an AF prediction prior to the conformational sampling

Downloaded from academic.oup.com/nar/article/54/W1/W216/8662889 by guest on 17 November 2026

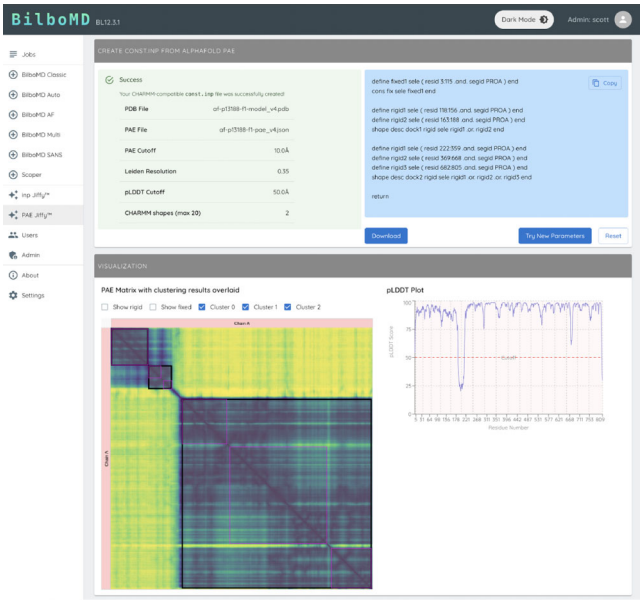

Figure 3. A screenshot of the PAE Jiffy output showing the CHARMM-compatible constraint definitions in the upper right. The input AlphaFold PAE matrix is shown in the lower left corner with calculated rigid domains indicated by overlaid square regions. A plot of per-residue local confidence score (pLDDT) is also shown in the lower-right panel, with the cutoff indicated by a dashed line.

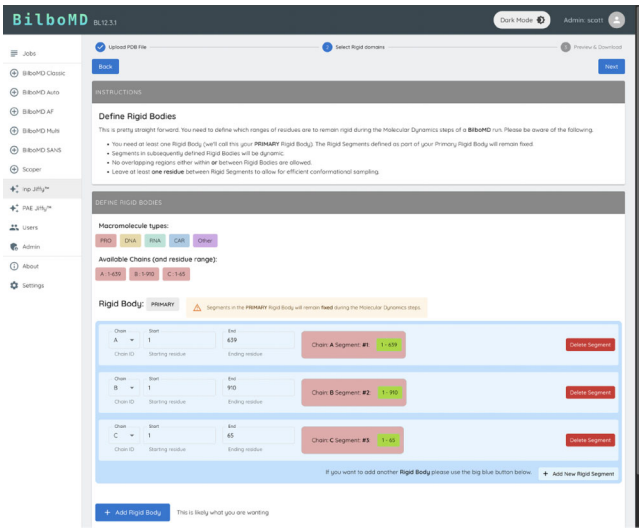

Figure 4. A screenshot of the BilboMD Inp Jiffy showing the step where users can interactively define rigid bodies.

step. The BilboMD Classic pipeline requires the user to prepare all inputs: an initial model (which can come from any source—including other structure prediction or modeling programs), 3-column SAXS data, and an MD constraint file (typically named `const.inp`). The BilboMD Auto pipeline assumes that a user has already run AlphaFold2/AlphaFold3 on their own and will supply a starting AlphaFold PDB model and the AlphaFold PAE matrix file. Although a user may provide an experimentally determined structure or a model from AF [23, 24] or RoseTTAFold [27], these models often lack flexible regions and require supplementation with a tool such as MODELER [28]. BilboMD Classic includes the conversion of PDBs to a CHARMM-compatible coordinate file (`*.crd`) and protein structure file (`*.psf`). The generation of the MD constraint file (`const.inp`), which defines rigid and flexible regions, can be done automatically from the predicted aligned error (PAE) matrix produced by AF using PAE Jiffy, our web-based tool designed to enable rapid ("in a jiffy") generation of constraint files (Fig. 3), or manually via Inp Jiffy (Fig. 4).

The experimental SAXS curve should be in three-column format with a scattering vector q (in Å^{-1} unit defined as: $q = 4\pi\sin\theta/\lambda$, where 2θ is the scattering angle), scattering intensity, and experimental error. BilboMD validates the data format, particularly the q format, and informs the user whether it is compatible with subsequent SAXS fitting. Although significant effort has gone into developing and testing the validation code, there may be cases of perfectly valid SAXS data that are rejected or invalid data that is accepted. We encourage users to contact us if they run into data validation issues.

Definition of rigid and flexible regions

The Inp Jiffy was created to provide a fully interactive experience. It features a multipart form that guides the user through the entire process of defining rigid domains and bodies (Fig. 4). The Inp Jiffy includes robust validation and syntax checking, ensuring that the resulting constraint definitions are fully compatible with CHARMM.

Defining the rigid and flexible regions of the starting atomic model is critical for subsequent MD steps to productively create the ensemble of possible conformations. These definitions can be made manually by more advanced users with a deep understanding of their system or automatically. The BilboMD web app provides two user-interactive Jiffys to guide users in this step (Inp and PAE Jiffy).

The PAE Jiffy (inspired by the ChimeraX AlphaFold Error Plot visualization tool [29]) is an automated tool for generating a constraint file. It uses an AF model combined with the AF PAE matrix and pLDDT. It produces a CHARMM-compatible selection of rigid and flexible regions in the form of a `const.inp` file, along with visualization artifacts that enhance feedback quality for the user (Fig. 3). Rigid and flexible regions are detected using the Leiden clustering algorithm [30], implemented in the igraph Python package, yielding a CHARMM-compatible input file that can be reviewed and customized by the user before being included in a BilboMD Classic run. After parsing the structure coordinate file to map residues, chains, and pLDDT, the code validates that the PAE matrix is square and consistent with the length of the input structure. It then converts PAE values (Å) into a similarity graph using either an exponential kernel $S = \exp(-(\text{PAE}/\sigma)^2)$ or a linear transform $S = \max(0, 1 - \text{PAE}/T)$. There are several options to modify the behavior of the PAE Jiffy algorithm when running the Python code on the command line. Currently, only three of these options are exposed in the front-end user interface. These include the global PAE cutoff (`–pae_cutoff`), which controls how permissive the graph is when connecting residues. Residue pairs with PAE values below this cutoff are considered linked in the clustering graph; pairs above it are ignored. The Leiden resolution (`–leiden_resolution`) controls the granularity of rigid region detection. We also introduce a third user-definable input option, pLDDT Cutoff (`–plddt_cutoff`), to filter clusters based on their average pLDDT values. The Jiffy enforces a minimum segment length of 10 residues, coalesces

Downloaded from academic.oup.com/nar/article/54/W1/W216/8662889 by guest on 17 November 2026

overlapping clusters, and guarantees at least a two-residue gap between adjacent domains on the same chain. Finally, segment identifiers are normalized to match CHARMM segments, and outputs are written deterministically, allowing users to visually review domain maps and use the generated constraints (`const.inp`) directly in the BilboMD Classic pipeline.

Conformational sampling and SAXS fitting

BilboMD employs a simplified MD strategy to efficiently explore conformational ensembles consistent with experimental SAXS data. Rather than modeling every atomic interaction, the system employs a reduced representation in which rigid and flexible regions (defined by user-supplied or PAE-derived constraint files) constrain the degrees of freedom during the simulation. Rigid domains are treated as internally frozen bodies, while flexible regions are modeled using standard bonded and non-bonded interactions. This significantly reduces the number of variables and allows the model to explore as many conformations as possible.

To overview, the structure is energy-minimized; the flexible regions are then heated to 600–1500K and subjected to an MD simulation with SAXS-derived radius of gyration (R_g) constraints. The R_g is automatically determined using a comprehensive Guinier analysis that scans all possible q-range windows in the experimental SAXS data. For each window containing at least 10 data points, a weighted linear regression is performed on $\ln(I)$ versus q^2, and the fit is validated against multiple criteria: $R^2 \geq 0.90$, negative slope (physical requirement), and qR_g within the Guinier region (0.3–1.3). The algorithm selects the optimal fit by maximizing R^2, with preference for windows with more data points when R^2 values are comparable, and calculates $R_g = \sqrt{(-3m)}$ from the regression slope. This automated approach ensures robust R_g determination across diverse molecular systems without manual intervention.

Historically, we have depended on CHARMM [31, 32] for all MD steps, including conformational sampling. However, we have recently developed a variant of BilboMD that uses OpenMM [25], compatible with GPU computing capabilities. As mentioned, the simulations are restrained by SAXS-derived R_g values, which bias sampling toward conformations whose overall size matches experimental scattering data. These restraints are applied as harmonic potentials centered on the experimental R_g, ensuring that the trajectory explores physically realistic structures.

BilboMD performs conformational sampling using either CHARMM or OpenMM, automatically applying the appropriate force field and constraint syntax. The simplified MD approach generates a large, statistically relevant pool of conformers in a fraction of the time required for all-atom simulations, while maintaining fidelity to both structural and experimental observables [12]. A pool of candidate conformers is extracted from the MD trajectory and the theoretical SAXS curves pre-calculated with FoXS [9, 11]. Candidate models and model ensembles are subsequently fitted to experimental data using MultiFoXS [33] to identify the best-scoring ensemble model. Finally, BilboMD aggregates key outputs (fits, residuals, R_g/D_{max} summaries, selected structures), provides user-friendly summaries/visualizations to aid interpretation, and, for registered users, notifies them by email when the job is complete. If the user feedback report suggests increasing the sampling/flexibility or if system is known to contain an intrinsically disordered protein (IDP), the user may run multiple BilboMD runs with various R_g ranges and combine them with MultiFoXS as implemented in BilboMD Multi pipeline.

User feedback report

A feedback report is implemented to summarize the quality of users' results and provide advice on improving model fit, if needed. First, the optimal number of states for the ensemble is determined and used in the feedback report. This is done based on the goodness-of-fit of each ensemble model. The optimal number of states is taken to be the lowest value at which χ^2 does not decrease significantly (20%) when more states are added to the ensemble, which would indicate the need for additional conformations to optimally fit the data.

An important initial check is to compare the molecular weight (MW) of the experimental SAXS curve with the theoretical MW from the model calculated from a power law adjustment of the volume of correlation (V_c). This can immediately detect common mistakes detrimental to analysis, namely, sample aggregation, oligomerization, or the use of the incorrect sequence. When a large discrepancy between the model MW and the experimental MW exists, the user should reconsider either their SAXS curve or their model. If MW is within acceptable error, the summary section will instead describe the model fit quality.

While the goodness-of-fit of the overall SAXS curve is optimized during conformational modeling, it is vital to examine χ^2 as a function of q to assess the quality of the model fit. Examining goodness-of-fit in specific q-ranges which we categorize as low, mid, and high-q within the SAXS curve can suggest how to improve the model. If only some of these regions exhibit poor goodness-of-fit, whereas others fit well, the model can likely be improved by adjusting the MD constraints. The PAE Jiffy or manual adjustment of the `const.inp` file can be used to redefine constraints based on the feedback report.

Poor fits at low q ($< 0.1\text{Å}^{-1}$) indicate incorrect domain grouping or positioning, assuming MW matches the model. In this case, users should alter the constraints to adjust interdomain grouping or interface binding. Complications associated with a poor MW match will also likely cause low-q error to be high (incorrect sequence, small amounts of oligomerization, or aggregation). Mid-q ($0.1 < q < 0.2\text{Å}^{-1}$) is highly dependent on the flexibility and movement of linkers. A poor mid-q fit strongly suggests that the model will need greater movement and thus a larger number of flexible residues during conformational fitting. High q ($> 0.2\text{Å}^{-1}$) is the least likely to fit poorly, but high error in this region may indicate poor background subtraction. In this case, users should revisit their subtraction method. Sidechain and hydration-layer effects may also affect the fit of this region if noise is sufficiently low enough to capture these features. If all three regions have sufficiently low χ^2 values and zero residuals, the user may consider the model a reasonable representation of the solution state. The feedback report establishes $\chi^2 < 2.0$ as a good fit. However, it is difficult to declare a universal cutoff of an acceptable χ^2 as the interpretation of χ^2 can vary. It is more likely to be higher for complex systems, but can also be artificially lower if noise is high. We recommend using χ^2 to evaluate how conformational sampling improved the model fit or when comparing jobs with different constraints.

Downloaded from academic.oup.com/nar/article/54/W1/W216/8662889 by guest on 17 November 2026

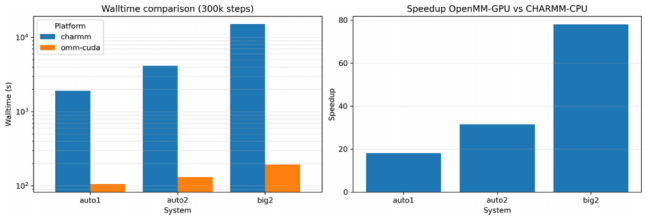

Figure 5. Comparison of wall time and resulting speedup for OpenMM (using GPU) versus CHARMM (using CPU) for three different test systems. auto1 is an AF predicted structure of arginyl-tRNA protein transferase 1. auto2 is an AF predicted structure of glutamine-tRNA ligase, and big2 is a 15 000-atom protein system.

Results

OpenMM versus CHARMM

BilboMD was originally developed to use CHARMM MD, as it provides several features for dealing with rigid bodies (CHARMM keyword `SHAPe`) and radius of gyration (R_g) restraints (CHARMM keyword `RGYRation`), which are not readily available in other MD packages. Several routines in CHARMM incorporate GPU support; however, in our experience, detailed expertise in CHARMM was required to rewrite CHARMM scripts to enable GPU support, which was not readily available to us. Thus, as an alternative, we adapted the BilboMD pipelines to use OpenMM [25], a high-performance toolkit for molecular simulation that provides GPU support and includes extensive language bindings for Python, C, C++, and Fortran. Additionally, the original BilboMD inputs for CHARMM enabled MD features, balancing the computational workload and relative impact on accuracy given the resolution required for comparison with experimental SAXS data. With the availability of GPUs, running a more detailed set of inter-particle calculations is possible in a reasonable wall time, and we experimented with this approach for our OpenMM runs. In our tests, multi-state models resulting from BilboMD CHARMM and OpenMM runs are essentially identical (Supplementary Fig. S1). Our observations are consistent with those from work describing a detailed comparison of multiple MD packages, showing that "most programs agree quite well, probably enough for most practical purposes" [34].

The wall time and speedup between OpenMM and CHARMM for the computationally intensive MD step (excluding minimization and heating) were measured across three test systems (Fig. 5). The measurements were performed on the NERSC Perlmutter supercomputing system using AMD EPYC 7763 Milan CPUs and NVIDIA A100 (40GB) GPUs. The MD simulations were run for 300 000 steps each and used a single R_g value for each system. For OpenMM, 8% of the wall time was required for simulation setup (including JIT time and other associated GPU setup). The memory footprint for the largest test system (15 000 atoms) was 500 MB; we did not need to scale to multiple GPUs per system, which is readily enabled via OpenMM if required. The wall times for OpenMM are one to two orders of magnitude lower than those required by CHARMM for these test systems, and the resulting speedups were 18×, 31×, and 78×. It is possible to run multiple simulations concurrently on a node, and if we assume "n" as a typical number of R_gs runs per system, utilizing the 4 GPUs per Perlmutter node (one GPU per R_g) decreases the measured raw speedups by a factor of n/4 assuming all CPU runs can be performed concurrently; however, since n is typically 6–12, BilboMD with OpenMM runs are still expected to be appreciably faster as compared to BilboMD using CHARMM runs on Perlmutter. We note again that CHARMM is currently configured to run with restricted inter-particle interactions (CHARMM keyword `NOElec`) and one CPU thread, whereas OpenMM is currently configured to use one GPU per system and to calculate additional inter-particle forces (e.g. electrostatics), thereby increasing the computational workload. A detailed study balancing performance, accuracy, and validation may be beneficial for optimizing future BilboMD runs.

Extensibility

The modular design of BilboMD enables the integration of new computational pipelines and analysis modules with minimal modification to the core system. Each pipeline is defined as a sequence of reusable steps that share a consistent API for job submission, monitoring, and data exchange. This architecture makes it straightforward to extend the platform beyond the original BilboMD SAXS-focused workflows to include new modeling strategies, such as combining multiple BilboMD runs with various starting models and SAXS curves using MultiFoXS as implemented in BilboMD Multi, or fitting SANS data (BilboMD SANS). Additional tools, such as SCOPER for AI-driven SAXS-validated RNA modeling [20] or future AI-based refinement modules, can be incorporated by registering new worker tasks and corresponding frontend forms, ensuring that BilboMD can evolve in parallel with emerging methods in structural biology while maintaining reproducibility and interoperability across environments.

User experience

Before submitting a BilboMD job, users have two tools: Inp Jiffy and PAE Jiffy, available to assist them in preparing CHARMM-compatible constraint files that define rigid and flexible regions (Figs 1 and 2). The Inp Jiffy helps construct a valid `const.inp` file directly from PDB coordinates, requires that chain identifiers be present, and automatically produces segment names compatible with the BilboMD Classic pipeline. The PAE Jiffy streamlines this process further by leveraging AF outputs: a predicted structure (PDB) and its corresponding PAE, in JSON format.

Job submission is handled via structured forms with contextual help and validation, including required file types (e.g. SAXS data and model coordinates) and numeric ranges for fit/MD parameters. Forms support multi-entity inputs for complex assemblies and preserve sensible defaults, making advanced options discoverable rather than mandatory. Large uploads and parameter sets are summarized before submission, and each run is tagged with user, time, and configuration metadata for downstream provenance.

After job submission, the user is presented with a job ID and a permalink URL that allows the job status and results to be viewed. When the modeling pipeline is complete, the analysis sections are displayed (Fig. 6). The results page will display plots comparing the fit of the initial and final ensemble models to experimental SAXS data, a Molstar structure viewer [35] (Fig. 7), and a download button for users to retrieve a bundled results file (`results.tar.gz`).

Downloaded from academic.oup.com/nar/article/54/W1/W216/8662889 by guest on 17 November 2026

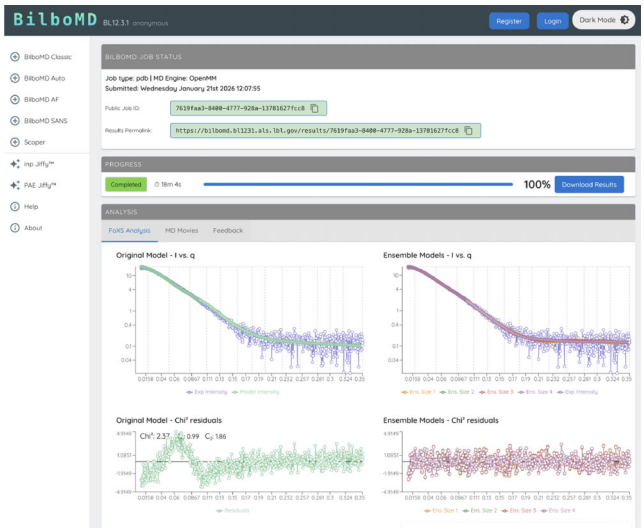

Figure 6. A screenshot showing the results page for a completed job. Basic information, including job ID, permalink URL along with before and after plots created by FoXS.

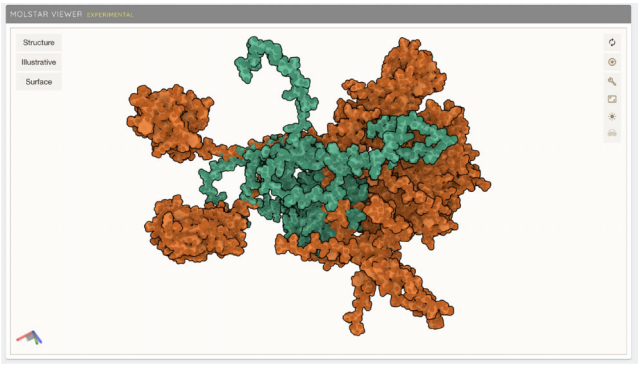

Figure 7. A screenshot showing the best ensemble model displayed in an embedded BilboMD Molstar viewer.

Case studies

We present examples of the BilboMD AF pipeline applied to SAXS data and protein sequences uploaded to SASBDB [36, 37]. We emphasize the use of the AF model, pLDDT, and PAE to generate constraints for rigid and flexible regions, facilitating conformational sampling. Additional BilboMD pipeline examples are shown in Supplementary Fig. S2.

Staphylococcal extracellular adherence protein

We demonstrate the BilboMD AF pipeline on Staphylococcal extracellular adherence protein (Eap) (SASBDB entry: SASDVF2) [38]. This protein consists of four domains connected like beads on a string, each classified as a rigid domain in the constraints (Fig. 8A). The AF model conformation fits the experimental SAXS data poorly (Fig. 8B), indicating solution flexibility. Intra-domain residues exhibit high pLDDT and low PAE values, while flexible regions show lower pLDDT and higher PAE values. The automatically defined `const.inp` file clearly identifies four Eap domains and a flexible linker. The 1-state model achieved $\chi^2 = 1.94$, while a 2-state model improved it to $\chi^2 = 1.17$. Increasing the number of states further does not significantly change the value of χ^2. Therefore, the 2-state ensemble was deemed the best model for the data, as

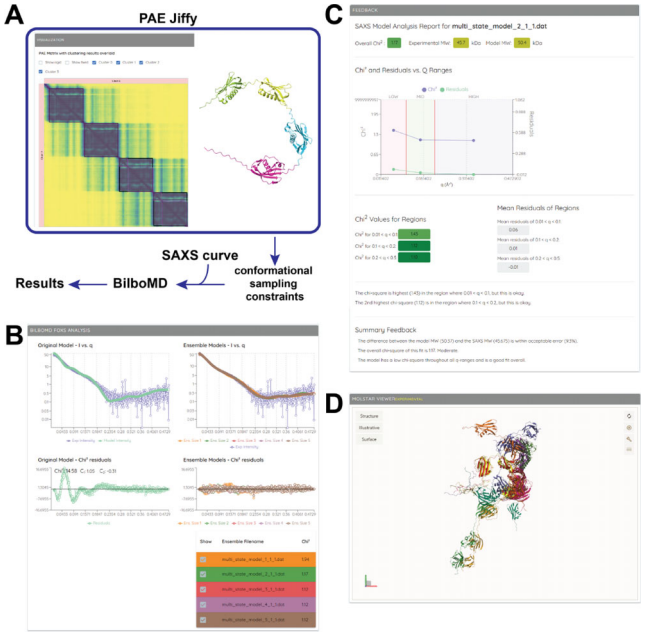

Figure 8. Example results of the BilboMD AF pipeline for a single chain protein, staphylococcal extracellular adherence protein in unbound form (SASDVF2). (**A**) Determination of restraints using the PAE Jiffy for BilboMD conformational sampling. (**B**) FoXS analysis to determine goodness-of-fit for ensemble states. (**C**) Feedback report of BilboMD job. (**D**) Molstar model viewer.

indicated by the feedback panel (Fig. 8C). This demonstrates the flexible behavior of the Eap domains, which are illustrated in the model viewer (Fig. 8D).

Serine/threonine-protein phosphatase (PP1) bound to protein phosphatase 1 (PTG)

We applied the BilboMD AF pipeline on serine/threonine-protein phosphatase (PP1) bound to protein phosphatase 1 (PTG), a two-chain multidomain structure (SASBDB entry: SASDNF2) [39]. The constraints file for this protein consisted of two primary rigid domains. One of these domains is interchain and contains the majority of PP1 and residues 16–42 of PTG, corresponding to an associated region. The other domain contains a larger portion of PTG (Fig. 9A). BilboMD achieved a 2-state ensemble with $\chi^2 = 0.98$ (Fig. 9B), capturing the dynamics of the two rigid domains.

Aggregated sample

A third example highlights a sample that could not be improved by BilboMD. The feedback panel shows that the molecular weight calculated from the SAXS is very high (Fig. 10C). This indicates that there was major aggregation during the SAXS measurement, which is also visible in the SAXS curve (Fig. 10A). In this case, SAXS cannot resolve the solution-state conformation of individual particles.

Web app architecture and components

For the web-based user interface, we chose a modern JavaScript stack centered on React with Material-UI (MUI) components and RTK Query for state management and data fetching. React offers a flexible, widely adopted framework for creating interactive single-page applications, while MUI provides a robust library of accessible, responsive

Downloaded from academic.oup.com/nar/article/54/W1/W216/8662889 by guest on 17 November 2026

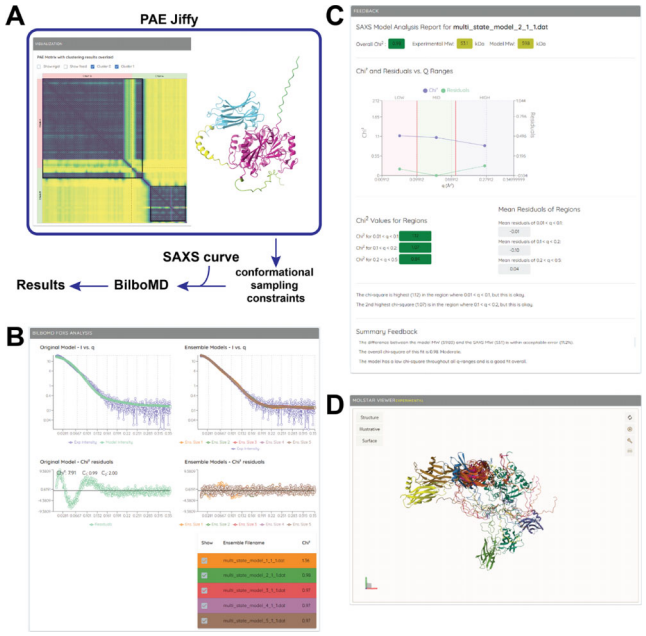

Figure 9. Example results of the BilboMD AF pipeline for a two-chain, multi-domain protein, serine/threonine-protein phosphatase (PP1) bound to protein phosphatase 1 (PTG) (SASDNF2). (**A**) Determination of restraints using the PAE Jiffy for BilboMD conformational sampling. (**B**) FoXS analysis to determine goodness-of-fit for ensemble states. (**C**) Feedback report of BilboMD job. (**D**) Molstar model viewer.

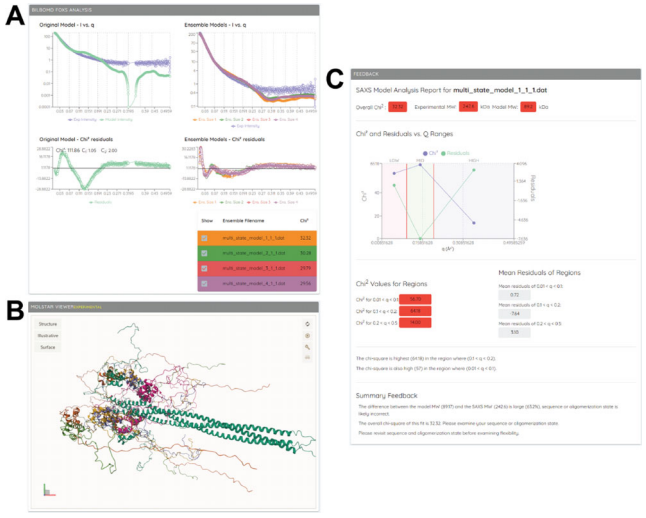

Figure 10. Example results of a BilboMD job using a SAXS curve that indicated sample aggregation. (**A**) FoXS analysis to determine goodness-of-fit for ensemble states. (**B**) Molstar model viewer. (**C**) Feedback report of the BilboMD job.

components that ensure a consistent user experience across platforms. RTK Query integrates seamlessly with Redux Toolkit to simplify data synchronization between the frontend and backend, reducing boilerplate code and enhancing maintainability. Overall, this stack enables us to deliver a clean, efficient, and scalable interface that allows users to submit jobs, monitor progress, and visualize SAXS modeling results without requiring specialized local software.

The backend is implemented in TypeScript/Node.js using Express to expose a versioned REST API with OpenAPI/Swagger documentation. Persistent data are stored in MongoDB (accessed via Mongoose), with Redis and BullMQ providing job queuing and progress tracking for asynchronous pipelines. A companion worker layer (Node.js and selected Python microservices for SAXS/MD steps) executes containerized tasks, including Slurm/Podman-HPC submissions at NERSC via the Superfacility API. Authentication (optional) is provided via one-time passwords sent via email. Enhancements to optional authentication are underway to enable ORCID OAuth. Rate limiting, request logging, and JSON-structured logs aid in debugging and monitoring. Individual BilboMD services are packaged with Docker and deployed either via Kubernetes/Helm (as implemented at NERSC on their Rancher/SPIN system) or via Docker Compose to the local SIBYLS beamline hardware, ensuring reproducibility, horizontal scaling, and controlled versioning across environments (Supplementary Fig. S3).

Discussion

The integration of computational structure prediction with experimental SAXS has become a key aspect of modern structural biology [40, 41]. SAXS provides a crucial link between atomistic models—such as those generated by AlphaFold [42–44] or RoseTTAFold [45–47]—and experimental data. It provides quantitative insights into molecular size, shape, and conformational diversity under near-physiological conditions, making it an ideal method for assessing the consistency of predicted structures [48–51].

With the release of AlphaFold3 and RoseTTAFold3, the accuracy of *de novo* protein structure prediction has significantly improved, often reaching near-experimental precision for monomeric and well-folded domains. However, despite the high local accuracy of AlphaFold predictions, discrepancies frequently arise when comparing predicted structures with experimental SAXS profiles. These discrepancies result from intrinsic flexibility, multi-domain rearrangements, conformational ensembles, or errors in the relative positioning of domains [38, 49, 51, 52]. SAXS, therefore, becomes an essential tool for assessing the solution-state validity of AlphaFold models, highlighting deviations that may not be apparent from global PAE or local pLDDT metrics.

Accurate SAXS profile calculators such as FoXS, CRYSOL, Pepsi-SAXS, and WAXSiS [10, 11, 53, 54] allow direct comparison between experimental SAXS data and predicted models by assessing the goodness-of-fit with parameters like χ^2 or correlation coefficients [55]. Importantly, these calculators can include hydration-layer effects, excluded-volume corrections, and flexible fitting routines, thereby supporting meaningful interpretation even for complex or partially disordered systems.

Combining AI-predicted models with experimental SAXS data suggests a workflow: (i) generate candidate structures using AI-driven structural prediction, (ii) calculate theoretical SAXS curves, and (iii) refine or filter the models based on how well they match experimental SAXS data. This approach can also assist in reconstructing multi-domain arrangements or conformational ensembles that single static predictions do not capture by applying ensemble-rigid-body modeling tools such as BilboMD v1, MultiFoXS, EOM, and Sassie [12, 33, 56, 57]. This workflow accommodates SAXS data within a population-based representation of conformational heterogeneity.

Downloaded from academic.oup.com/nar/article/54/W1/W216/8662889 by guest on 17 November 2026

However, none of these methods directly incorporates AlphaFold statistical information from the PAE and pLDDT scores, and the selection of flexible regions is based on visual inspection of predicted structures [43]. The recent application of SAXS-A-FOLD [42] demonstrates the potential of using the pLDDT value to identify flexible regions and guide ensemble modeling. However, this application only accepts single-chain proteins and does not incorporate global PAE-derived constraints. Additionally, current methods for deriving ensemble models involve multiple steps, including structure prediction, definition of flexibility restraints, conformational sampling, SAXS fitting, and ensemble formation. Our BilboMD web application extends this framework by automatically determining rigid and flexible regions in the BilboMD AF modeling pipeline.

Several challenges remain. The sensitivity of SAXS to flexible and disordered regions often makes direct fitting difficult, especially when AlphaFold predicts compact conformations for intrinsically disordered proteins. It is, however, possible to model IDPs with BilboMD. In a recent study, BilboMD was used to model the highly disordered protein Sca2 from *Rickettsia bellii*, which validated the minimal fold predicted by AlphaFold3 [48]. Likewise, SAXS data alone cannot reveal local structural details, highlighting the need to combine it with complementary information from cryo-EM, NMR, or crosslinking mass spectrometry. Furthermore, while current SAXS calculators approximate solvent and hydration effects well, differences in modeling hydration shells or partial disorder can cause systematic deviations between calculated and experimental profiles [58–60]. Despite these limitations, the combination of AlphaFold and SAXS offers a powerful approach for solution-state structural validation. By linking atomistic predictions with experimental data, SAXS not only enhances confidence in predicted conformations but also reveals biologically important flexibility that static computational models often overlook. As computational prediction methods improve and SAXS calculators become more accurate and accessible, this combined strategy is likely to play an even larger role in integrative structural biology, particularly in exploring dynamic assemblies, conformational changes, and protein–nucleic acid complexes that are essential to cellular function.

Integrative SAXS and SANS modeling provides a powerful framework for refining AI-driven structural predictions and ensuring their experimental and real-world validity. In this context, BilboMD generates experimentally validated models that deliver mechanistic insights to accelerate discovery across academic, industrial, and government research.

Acknowledgements

We are grateful for the patience of our early users who were willing to work with us to identify bugs and suggest improvements in usability and functionality. Their feedback was essential in shaping BilboMD into a more robust and accessible tool. We thank the reviewers who provided valuable feedback while preparing the manuscript. We thank our colleagues at the Advanced Light Source and other synchrotron facilities for valuable discussions on SAXS workflows and integration into experimental pipelines. Deployment of BilboMD to NERSC was made possible by support from the NERSC SPIN team (with special thanks to Nicholas Tyler and Gabor Torok) and the NESAP program (with assistance from Johannes Blaschke), whose guidance on container orchestration and high-performance computing integration greatly facilitated this work. We also acknowledge the developers of all the open-source software libraries and packages that form the foundation of BilboMD, and the funding agencies whose continued support of data-driven structural biology enabled the development of this resource.

Author contributions: Scott Classen (Conceptualization [equal], Methodology [equal], Software [lead], Supervision [lead], Writing—original draft [equal]), Joshua Del Mundo (Methodology [supporting], Software [supporting], Validation [equal], Writing—original draft [equal]), Dhruva Kulkarni (Methodology [supporting], Writing—original draft [equal]), Shreyas Prabhakar (Methodology [supporting], Software [supporting]), Alan Hicks (Software [supporting]), and Michal Hammel (Conceptualization [equal], Methodology [equal], Software [supporting], Validation [equal], Writing—original draft [equal])

Supplementary data

Supplementary data is available at NAR online.

Conflict of interest

None declared.

Funding

Development of BilboMD and collection of experimental SAXS data were performed at the Advanced Light Source (ALS) at the SIBYLS beamline, a national user facility operated by Lawrence Berkeley National Laboratory on behalf of the Department of Energy, Office of Basic Energy Sciences, through the Integrated Diffraction Analysis Technologies (IDAT) program, supported by DOE Office of Biological and Environmental Research. Additional support comes from the National Institute of Health project ALS-ENABLE (P30 GM124169). Efforts to apply SAXS and MX to characterize eukaryotic pathways relevant to human cancers are supported in part by the National Cancer Institute grant Structural Biology of DNA Repair (SBDR) CA92584. S.C. and M.H. were funded, in part, by the Advanced Research Projects Agency for Health (ARPA-H). This research used resources of the National Energy Research Scientific Computing Center (NERSC), a Department of Energy User Facility using NERSC award DDR-ERCAP0031203.

Data availability

All code for the BilboMD is available on GitHub (github.com/bl1231/bilbomd) and archived in Zenodo (doi.org/10.5281/zenodo.18319542). Two user-accessible BilboMD deployments are currently available. Both are free and open to all users, with no login required.

1. Deployed to the SIBYLS beamline compute infrastructure at https://bilbomd.bl1231.als.lbl.gov.
2. Deployed to NERSC at https://bilbomd-nersc.bl1231.als.lbl.gov.

References

1. Brosey CA, Tainer JA. Evolving SAXS versatility: solution X-ray scattering for macromolecular architecture, functional landscapes,

Downloaded from academic.oup.com/nar/article/54/W1/W216/8662889 by guest on 17 November 2026

and integrative structural biology. *Curr Opin Struc Biol* 2019;58:197–213. https://doi.org/10.1016/j.sbi.2019.04.004
2. Rambo RP, Tainer JA. Accurate assessment of mass, models and resolution by small-angle scattering. *Nature* 2013;496:477–81. https://doi.org/10.1038/nature12070
3. Semenyuk AV, Svergun DI. GNOM–a program package for small-angle scattering data processing. *J Appl Crystallogr* 1991;24:537–40. https://doi.org/10.1107/S002188989100081X
4. Hura GL, Menon AL, Hammel M *et al.* Robust, high-throughput solution structural analyses by small angle X-ray scattering (SAXS). *Nat Methods* 2009;6:606–12. https://doi.org/10.1038/nmeth.1353
5. Classen S, Hura GL, Holton JM *et al.* Implementation and performance of SIBYLS: a dual endstation small-angle X-ray scattering and macromolecular crystallography beamline at the Advanced Light Source. *J Appl Crystallogr* 2013;46:1–13. https://doi.org/10.1107/S0021889812048698
6. Rosenberg DJ, Hura GL, Hammel M. Size exclusion chromatography coupled small angle X-ray scattering with tandem multiangle light scattering at the SIBYLS beamline. *Methods Enzymol* 2022;677:191–219. https://doi.org/10.1016/bs.mie.2022.08.031
7. Dyer KN, Hammel M, Rambo RP *et al.* High-throughput SAXS for the characterization of biomolecules in solution: a practical approach. *Methods Mol Biol* 2014;1091:245–58. https://doi.org/10.1007/978-1-62703-691-7_18
8. Brosey CA, Link TM, Shen R *et al.* Chemical screening by time-resolved X-ray scattering to discover allosteric probes. *Nat Chem Biol* 2024;20:1199–209. https://doi.org/10.1038/s41589-024-01609-1
9. Schneidman-Duhovny D, Hammel M, Tainer JA *et al.* Accurate SAXS profile computation and its assessment by contrast variation experiments. *Biophys J* 2013;105:962–74. https://doi.org/10.1016/j.bpj.2013.07.020
10. Svergun D, Barberato C, Koch MHJ. CRYSOL—a program to evaluate X-ray solution scattering of biological macromolecules from atomic coordinates. *J Appl Crystallogr* 1995;28:768–73. https://doi.org/10.1107/S0021889895007047
11. Schneidman-Duhovny D, Hammel M, Sali A. FoXS: a web server for rapid computation and fitting of SAXS profiles. *Nucleic Acids Res* 2010;38:W540–44. https://doi.org/10.1093/nar/gkq461
12. Pelikan M, Hura GL, Hammel M. Structure and flexibility within proteins as identified through small angle X-ray scattering. *Gen Physiol Biophys* 2009;28:174–89. https://doi.org/10.4149/gpb_2009_02_174
13. Hub JS. Interpreting solution X-ray scattering data using molecular simulations. *Curr Opin Struc Biol* 2018;49:18–26. https://doi.org/10.1016/j.sbi.2017.11.002
14. Hammel M. Validation of macromolecular flexibility in solution by small-angle X-ray scattering (SAXS). *Eur Biophys J: EBJ* 2012;41:789–99. https://doi.org/10.1007/s00249-012-0820-x
15. Schneidman-Duhovny D, Hammel M. Modeling structure and dynamics of protein complexes with SAXS profiles. *Methods Mol Biol* 2018;1764:449–73. https://doi.org/10.1007/978-1-4939-7759-8_29
16. Hammel M, Tainer JA. X-ray scattering reveals disordered linkers and dynamic interfaces in complexes and mechanisms for DNA double-strand break repair impacting cell and cancer biology. *Protein Sci* 2021;30:1735–56. https://doi.org/10.1002/pro.4133
17. Myers MJ, Xu Z, Ryan BJ *et al.* Molecular insights into the structure and function of the Staphylococcus aureus fatty acid kinase. *J Biol Chem* 2024;300:107920. https://doi.org/10.1016/j.jbc.2024.107920
18. Koduru T, Hantman N, Peters EV *et al.* A molten globule ensemble primes Arf1-GDP for the nucleotide switch. *Proc Natl Acad Sci USA* 2024;121:e2413100121. https://doi.org/10.1073/pnas.2413100121
19. Shimizu M, Tanaka H, Nishimura M *et al.* Asymmetric fluctuation of overlapping dinucleosome studied by cryoelectron microscopy and small-angle X-ray scattering. *PNAS Nexus* 2024;3:pgae484. https://doi.org/10.1093/pnasnexus/pgae484
20. Patt E, Classen S, Hammel M *et al.* Predicting RNA structure and dynamics with deep learning and solution scattering. *Biophys J* 2025;124:549–64. https://doi.org/10.1016/j.bpj.2024.12.024
21. Hopkins JB. BioXTAS RAW 2: new developments for a free open-source program for small-angle scattering data reduction and analysis. *J Appl Crystallogr* 2024;57:194–208. https://doi.org/10.1107/S1600576723011019
22. Franke D, Gräwert T, Svergun DI. New features in ATSAS-4, a program suite for small-angle scattering data analysis. *J Appl Crystallogr* 2025;58:1027–33. https://doi.org/10.1107/S1600576725002481
23. Jumper J, Evans R, Pritzel A *et al.* Highly accurate protein structure prediction with AlphaFold. *Nature* 2021;596:583–9. https://doi.org/10.1038/s41586-021-03819-2
24. Abramson J, Adler J, Dunger J *et al.* Accurate structure prediction of biomolecular interactions with AlphaFold 3. *Nature* 2024;630:493–500. https://doi.org/10.1038/s41586-024-07487-w
25. Eastman P, Galvelis R, Peláez RP *et al.* OpenMM 8: Molecular dynamics simulation with machine learning potentials. *J Phys Chem B* 2024;128:109–16. https://doi.org/10.1021/acs.jpcb.3c06662
26. Jo S, Kim T, Iyer VG *et al.* CHARMM-GUI: a web-based graphical user interface for CHARMM. *J Comput Chem* 2008;29:1859–65. https://doi.org/10.1002/jcc.20945
27. Baek M, DiMaio F, Anishchenko I *et al.* Accurate prediction of protein structures and interactions using a three-track neural network. *Science* 2021;373:871–6. https://doi.org/10.1126/science.abj8754
28. Webb B, Sali A. Comparative protein structure modeling using modeller. *Curr Protoc Bioinform* 2016;54:5.6.1–37. https://doi.org/10.1002/cpbi.3
29. Meng EC, Goddard TD, Pettersen EF *et al.* UCSF ChimeraX: tools for structure building and analysis. *Protein Sci* 2023;32:e4792. https://doi.org/10.1002/pro.4792
30. Traag VA, Waltman L, van Eck NJ. From Louvain to Leiden: guaranteeing well-connected communities. *Sci Rep* 2019;9:5233. https://doi.org/10.1038/s41598-019-41695-z
31. Brooks BR, Brooks CL, Mackerell AD *et al.* CHARMM: the biomolecular simulation program. *J Comput Chem* 2009;30:1545–614. https://doi.org/10.1002/jcc.21287
32. Hwang W, Austin SL, Blondel A *et al.* CHARMM at 45: enhancements in accessibility, functionality, and speed. *J Phys Chem B* 2024;128:9976–10042. https://doi.org/10.1021/acs.jpcb.4c04100
33. Schneidman-Duhovny D, Hammel M, Tainer JA *et al.* FoXS, FoXSDock and MultiFoXS: single-state and multi-state structural modeling of proteins and their complexes based on SAXS profiles. *Nucleic Acids Res* 2016;44:W424–9. https://doi.org/10.1093/nar/gkw389
34. Shirts MR, Klein C, Swails JM *et al.* Lessons learned from comparing molecular dynamics engines on the SAMPL5 dataset. *J Comput Aided Mol Design* 2017;31:147–61. https://doi.org/10.1007/s10822-016-9977-1
35. Sehnal D, Bittrich S, Deshpande M *et al.* Mol∗ Viewer: modern web app for 3D visualization and analysis of large biomolecular structures. *Nucleic Acids Res* 2021;49:W431–7. https://doi.org/10.1093/nar/gkab314
36. Kikhney AG, Borges CR, Molodenskiy DS *et al.* SASBDB: towards an automatically curated and validated repository for biological scattering data. *Protein Sci* 2020;29:66–75. https://doi.org/10.1002/pro.3731
37. Blanchet CE, Sutinen A, Graewert MA *et al.* SASBDB reaches 5000 data sets: empowering open science and next-generation SAS analysis. *Acta Crystallogr D Struct Biol* 2026;82:151–4. https://doi.org/10.1107/S2059798326000641

Downloaded from academic.oup.com/nar/article/54/W1/W216/8662889 by guest on 17 November 2026

38. Mishra N, Gido CD, Herdendorf TJ *et al. S. aureus* Eap is a polyvalent inhibitor of neutrophil serine proteases. *J Biol Chem* 2024;300:107627. https://doi.org/10.1016/j.jbc.2024.107627
39. Semrau MS, Giachin G, Covaceuszach S *et al.* Molecular architecture of the glycogen- committed PP1/PTG holoenzyme. *Nat Commun* 2022;13:6199. https://doi.org/10.1038/s41467-022-33693-z
40. Ogorzalek TL, Hura GL, Belsom A *et al.* Small angle X-ray scattering and cross-linking for data assisted protein structure prediction in CASP 12 with prospects for improved accuracy. *Proteins* 2018;86:202–14. https://doi.org/10.1002/prot.25452
41. Hura GL, Hodge CD, Rosenberg D *et al.* Small angle X-ray scattering-assisted protein structure prediction in CASP13 and emergence of solution structure differences. *Proteins* 2019;87:1298–314. https://doi.org/10.1002/prot.25827
42. Brookes E, Curtis JE, Householder A *et al.* SAXS-A-FOLD: a website for fast ensemble modeling optimizing the fit of AlphaFold or user-supplied protein structures with flexible regions to SAXS data. *J Appl Crystallogr* 2025;58:1034–49. https://doi.org/10.1107/S1600576725003590
43. Brookes E, Rocco M, Vachette P *et al.* AlphaFold-predicted protein structures and small-angle X-ray scattering: insights from an extended examination of selected data in the Small-Angle Scattering Biological Data Bank. *J Appl Crystallogr* 2023;56:910–26. https://doi.org/10.1107/S1600576723005344
44. Receveur-Bréchot V. AlphaFold, small-angle X-ray scattering and ensemble modelling: a winning combination for intrinsically disordered proteins. *J Appl Crystallogr* 2023;56:1313–4. https://doi.org/10.1107/S1600576723008403
45. Jiang H, Jude KM, Wu K *et al.* De novo design of buttressed loops for sculpting protein functions. *Nat Chem Biol* 2024;20:974–80. https://doi.org/10.1038/s41589-024-01632-2
46. Edman NI, Phal A, Redler RL *et al.* Modulation of FGF pathway signaling and vascular differentiation using designed oligomeric assemblies. *Cell* 2024;187:3726–40. https://doi.org/10.1016/j.cell.2024.05.025
47. Ben-Sasson AJ, Watson JL, Sheffler W *et al.* Design of biologically active binary protein 2D materials. *Nature* 2021;589:468–73. https://doi.org/10.1038/s41586-020-03120-8
48. Bacher MC, Choe JE, Jiang J *et al.* Divergent *Rickettsia* species exhibit distinct mechanisms of actin-based motility. bioRxiv, https://doi.org/10.1101/2025.08.14.669974, 22 August 2025, preprint: not peer reviewed.
49. Chinnam NB, Thapar R, Arvai AS *et al.* ASCC1 structures and bioinformatics reveal a novel helix-clasp-helix RNA-binding motif linked to a two-histidine phosphodiesterase. *J Biol Chem* 2024;300:107368. https://doi.org/10.1016/j.jbc.2024.107368
50. Tsai WJ, Lai YH, Shi YA *et al.* Structural basis underlying the synergism of NADase and SLO during group A Streptococcus infection. *Commun Biol* 2023;6:124. https://doi.org/10.1038/s42003-023-04502-0
51. Murray DT, Ge X, Schut GJ *et al.* Correlating conformational equilibria with catalysis in the electron bifurcating EtfABCX of *Thermotoga maritima*. *Biochemistry* 2024;63:128–40. https://doi.org/10.1021/acs.biochem.3c00472
52. McBride AC, Yu F, Cheng EH *et al.* Predicting pose distribution of protein domains connected by flexible linkers is an unsolved problem. *Proteins* 2025;94:362–80. https://doi.org/10.1002/prot.70062
53. Grudinin S, Garkavenko M, Kazennov A. Pepsi-SAXS: an adaptive method for rapid and accurate computation of small-angle X-ray scattering profiles. *Acta Crystallogr D Struct Biol* 2017;73:449–64. https://doi.org/10.1107/S2059798317005745
54. Knight CJ, Hub JS. WAXSiS: a web server for the calculation of SAXS/WAXS curves based on explicit-solvent molecular dynamics. *Nucleic Acids Res* 2015;43:W225–30. https://doi.org/10.1093/nar/gkv309
55. Hura GL, Budworth H, Dyer KN *et al.* Comprehensive macromolecular conformations mapped by quantitative SAXS analyses. *Nat Methods* 2013;10:453–4. https://doi.org/10.1038/nmeth.2453
56. Bernadó P, Mylonas E, Petoukhov MV *et al.* Structural characterization of flexible proteins using small-angle X-ray scattering. *J Am Chem Soc* 2007;129:5656–64. https://doi.org/10.1021/ja069124n
57. Curtis JE, Raghunandan S, Nanda H *et al.* SASSIE: a program to study intrinsically disordered biological molecules and macromolecular ensembles using experimental scattering restraints. *Comput Phys Commun* 2012;183:382–9. https://doi.org/10.1016/j.cpc.2011.09.010
58. Trewhella J, Vachette P, Bierma J *et al.* A round-robin approach provides a detailed assessment of biomolecular small-angle scattering data reproducibility and yields consensus curves for benchmarking. *Acta Crystallogr D Struct Biol* 2022;78:1315–36. https://doi.org/10.1107/S2059798322009184
59. Grishaev A, Guo L, Irving T *et al.* Improved fitting of solution X-ray scattering data to macromolecular structures and structural ensembles by explicit water modeling. *J Am Chem Soc* 2010;132:15484–6. https://doi.org/10.1021/ja106173n
60. Chen PC, Hub JS. Validating solution ensembles from molecular dynamics simulation by wide-angle X-ray scattering data. *Biophys J* 2014;107:435–47. https://doi.org/10.1016/j.bpj.2014.06.006

Received: February 5, 2026. **Revised:** March 26, 2026. **Accepted:** April 12, 2026
© The Author(s) 2026. Published by Oxford University Press.
This is an Open Access article distributed under the terms of the Creative Commons Attribution-NonCommercial License (https://creativecommons.org/licenses/by-nc/4.0/), which permits non-commercial re-use, distribution, and reproduction in any medium, provided the original work is properly cited. For commercial re-use, please contact reprints@oup.com for reprints and translation rights for reprints. All other permissions can be obtained through our RightsLink service via the Permissions link on the article page on our site—for further information please contact journals.permissions@oup.com.

Downloaded from academic.oup.com/nar/article/54/W1/W216/8662889 by guest on 17 November 2026